NASA/TM—2005–214192

Genesis Reentry Observations and Data Analysis

W.R. Swift
Raytheon, Huntsville, Alabama

R.M. Suggs
Marshall Space Flight Center, Marshall Space Flight Center, Alabama

November 2005

The NASA STI Program Office…in Profile

Since its founding, NASA has been dedicated to the advancement of aeronautics and space science. The NASA Scientific and Technical Information (STI) Program Office plays a key part in helping NASA maintain this important role.

The NASA STI Program Office is operated by Langley Research Center, the lead center for NASA's scientific and technical information. The NASA STI Program Office provides access to the NASA STI Database, the largest collection of aeronautical and space science STI in the world. The Program Office is also NASA's institutional mechanism for disseminating the results of its research and development activities. These results are published by NASA in the NASA STI Report Series, which includes the following report types:

- TECHNICAL PUBLICATION. Reports of completed research or a major significant phase of research that present the results of NASA programs and include extensive data or theoretical analysis. Includes compilations of significant scientific and technical data and information deemed to be of continuing reference value. NASA's counterpart of peer-reviewed formal professional papers but has less stringent limitations on manuscript length and extent of graphic presentations.

- TECHNICAL MEMORANDUM. Scientific and technical findings that are preliminary or of specialized interest, e.g., quick release reports, working papers, and bibliographies that contain minimal annotation. Does not contain extensive analysis.

- CONTRACTOR REPORT. Scientific and technical findings by NASA-sponsored contractors and grantees.

- CONFERENCE PUBLICATION. Collected papers from scientific and technical conferences, symposia, seminars, or other meetings sponsored or cosponsored by NASA.

- SPECIAL PUBLICATION. Scientific, technical, or historical information from NASA programs, projects, and mission, often concerned with subjects having substantial public interest.

- TECHNICAL TRANSLATION. English-language translations of foreign scientific and technical material pertinent to NASA's mission.

Specialized services that complement the STI Program Office's diverse offerings include creating custom thesauri, building customized databases, organizing and publishing research results…even providing videos.

For more information about the NASA STI Program Office, see the following:

- Access the NASA STI Program Home Page at ***http://www.sti.nasa.gov***

- E-mail your question via the Internet to help@sti.nasa.gov

- Fax your question to the NASA Access Help Desk at 301–621–0134

- Telephone the NASA Access Help Desk at 301–621–0390

- Write to:
  NASA Access Help Desk
  NASA Center for AeroSpace Information
  7121 Standard Drive
  Hanover, MD 21076–1320
  301–621–0390

NASA/TM—2005–214192

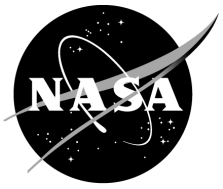

Genesis Reentry Observations and Data Analysis

W.R. Swift
Raytheon, Huntsville, Alabama

R.M. Suggs
Marshall Space Flight Center, Marshall Space Flight Center, Alabama

National Aeronautics and
Space Administration

Marshall Space Flight Center • MSFC, Alabama 35812

November 2005

Acknowledgments

The authors would like to thank Danielle Moser for her invaluable assistance during the planning, data collection, and analysis of these observations. Danielle was a member of the deployed team and without her hard work and attention to detail the observations would not have been successful. We also wish to thank the Space Shuttle Propulsion Systems Engineering and Integration Office at MSFC for supporting the project.

Available from:

NASA Center for AeroSpace Information
7121 Standard Drive
Hanover, MD 21076–1320
301–621–0390

National Technical Information Service
5285 Port Royal Road
Springfield, VA 22161
703–487–4650

TABLE OF CONTENTS

LIST OF FIGURES

LIST OF FIGURES (Continued)

LIST OF TABLES

LIST OF ACRONYMS

AVI	Audio Video Interleave
CW	continuous wave
DFT	discrete Fourier transform
EI	entry interface
FCC	Federal Communications Commission
FFT	fast Fourier transform
FOV	field of view
GPS	global positioning system
MSFC	Marshall Space Flight Center
TM	Technical Memorandum
UBVRI	ultraviolet, blue, visual, red, infrared
UT	universal time
VHF	very high frequency
VLF	very low frequency

TECHNICAL MEMORANDUM

GENESIS REENTRY OBSERVATIONS AND DATA ANALYSIS

1. INTRODUCTION

The Genesis spacecraft reentry represented a unique opportunity to observe a "calibrated meteor" from northern Nevada. Knowing its speed, mass, composition, and precise trajectory made it a good subject to test some of the algorithms used to determine meteoroid mass from observed brightness. It was also a good test of an inexpensive set of cameras that could be deployed to observe future shuttle reentries. The utility of consumer-grade video cameras was evident during the STS–107 accident investigation, and the Genesis reentry gave us the opportunity to specify and test commercially available cameras that could be used during future reentries. This Technical Memorandum (TM) describes the video observations and their analysis, compares the results with a simple photometric model, describes the forward scatter radar experiment, and lists lessons learned from the expedition and implications for the Stardust reentry in January 2006 as well as future shuttle reentries.

1.1 Prereentry Assumptions

Initial reentry expectations were as follows for September 8, 2004, from Wild Horse, NV:

- Acquisition: 15:55:28 UT
  Genesis capsule as bright as Venus at magnitude –4
  Marginally visible in daylight
  Altitude: 59 mi

- Brightness flare: 15:55:37 UT
  As bright as a typical iridium flare at magnitude –6
  Easily seen if you know where to look
  Altitude: 52.5 mi

- Maximum brightness: 15:56:04 UT
  Maximum brightness expected to be –9
  Same brightness as the last quarter Moon in the cameras
  Easily found and visible in daylight
  Altitude: 35 mi

- Rapid fading: 15:56:08 UT

1.2 Instrumentation

Two multiple camera arrays, a forward scatter radar receiver, and a very low frequency (VLF) receiver were deployed to the observing site and operated under remote power.

Cameras 1 through 5 were identical Astrovid StellacamEX video cameras with R25 red filters and linear polarization filters installed and aligned on each one to reduce the daylight sky background. The cameras were fitted with 12mm, f/0.8 wide-angle lenses and were aligned with a slight overlap to form a mosaic image with a field of view (FOV) over 100º in width. This array, dubbed "the Mosaic," was coupled with five Sony digital video recorders prewired into a carrying case and powered by a battery-powered inverter. It was intended to capture a continuous record essentially unattended. See figure 1.

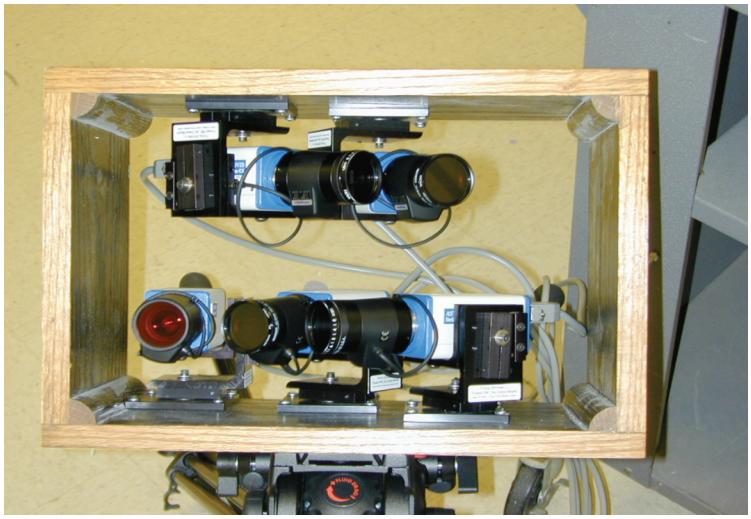

Figure 1. Mosaic camera array of five video cameras aligned to capture 110° FOV.

Cameras 6 through 10 were mounted coaligned in a box on a motion picture tripod with a riflescope arranged for tracking Genesis during reentry. This array was dubbed "the Tracker." Video cameras 6 through 9 were fitted with lenses of various focal lengths: camera 6—25mm with filters, camera 7—25mm with grating, camera 8—75mm with filters, and camera 9—400mm without filters. In each case the filters were an R25 red filter and a linear polarizer. See figures 2 and 3. Camera 10 was a Sony Handycam set to maximum optical zoom placed next to the riflescope to serve as an auxiliary sighting device at extreme elevation. It also served as an audio notebook.

Figure 2. Tracker video array at Wild Horse, NV. Tracking was never achieved due to low visibility of the Genesis capsule.

Figure 3. Tracker camera array fitted with lenses of various focal lengths and filters to reduce the daylight sky background.

The observing conditions for northern Nevada at the predicted reentry time were modeled using DayStar44 with ModTran4 and a catalog of filter, detector, and target spectra. DayStar44 is an enhanced version of Marshall Space Flight Center's (MSFC's) Natural Environments Branch video meteor analysis program, Meteor44, that is capable of modeling daylight sky radiation and atmospheric extinction. From this it was determined that a combination of an R25 red filter with a linear polarizer adjusted to reduce the sky background would make a significant difference (fig. 4). A preentry peak magnitude estimate by others of –9 visual—based on the assumption of 25 percent ablation—is not supported by the data, which indicates a peak somewhere around m_v –5.5 as shown here. (See figure 7 in section 2.2.) Although 4 magnitudes dimmer than predicted, the Genesis capsule was readily captured by the cameras and would have been easily visible in binoculars with an amber filter. Spectral considerations are further discussed in appendix A.

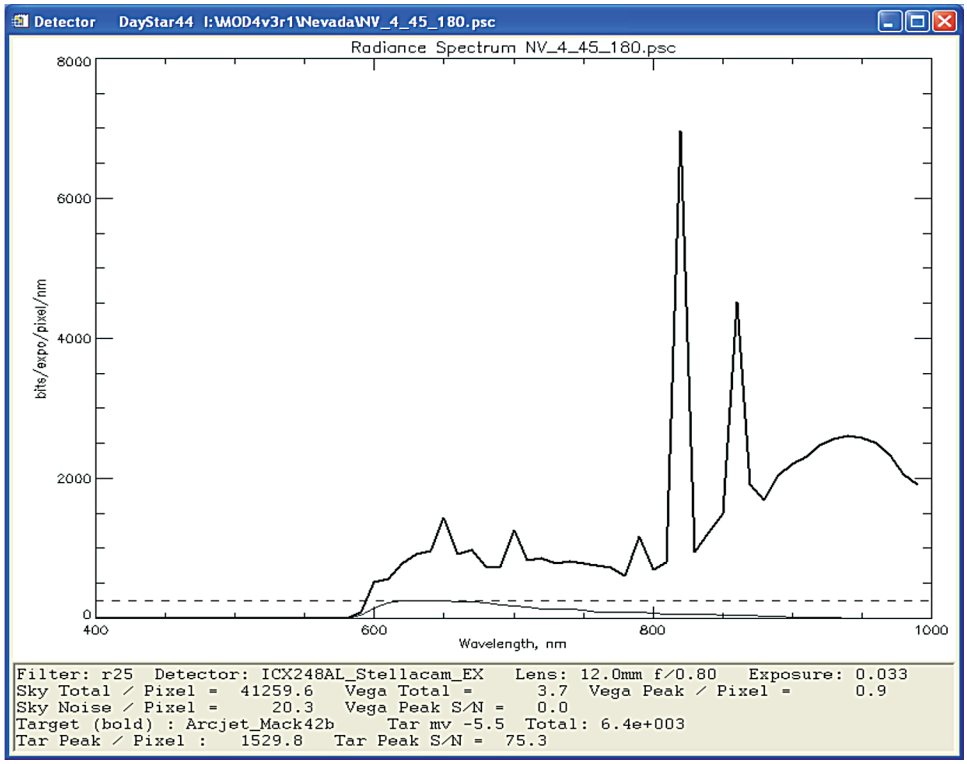

Figure 4. Calculated observations with R25 filter based on observed target visual magnitude of –5.5 with an arcjet plasma spectrum (bold). Also shown are the Vega m_v=0 reference (solid) and S/N=1 (dashed).

The forward scatter radar was based on a laptop computer with an Icom PCR1000 receiver set to 55.24 MHz or Ch 2(–). Simple rabbit ears were used as an antenna aligned northwest/southeast. The data were recorded by the laptop on the right audio channel. Carriers from Salt Lake City, UT; Klamath Falls, OR; Spokane, WA; and Billings, MT, were expected to be within range below the horizon.

The VLF receiver was a unit from The University of Western Ontario with a wire loop antenna pointed up. Its data were recorded on the laptop as well, but on the left channel. Radio and radar observations are discussed in detail later in this TM.

1.3 Observing Site

The day before Genesis' reentry was spent visiting the proposed observation site and examining the expected sight lines (fig. 5). A campsite at the Wild Horse Reservoir State Park, NV—global positioning system (GPS) coordinates 41°40.241´ N. 115° 48.135´ W., elevation 1,907 m—was chosen which had useful conveniences as well as the required clear FOV. This site was recommended by Bill Willcockson, the Lockheed-Martin Genesis Thermal Protection System manager, due to its proximity to the predicted maximum heating portion of the Genesis trajectory.

Figure 5. Mosaic camera array in position at Wild Horse Reservoir, NV. The reentry path was from far right (west) to the left in this view. Canadian VLF receiver and campsite is to the top left.

The night before reentry, the Mosaic camera was aligned with the predicted Genesis trajectory using appropriate star fields. A video was made of the star fields and the Moon for later calibration. VLF receiver antennas were deployed and the forward scatter radar was adjusted to record the reentry. Occasional meteors were noted. The morning dawned clear and cool with a slight haze that burned off later. Conditions were good for the reentry.

2. REENTRY OBSERVATIONS

Reentry acquisition was expected at 15:55:28 UT with initial brightness –4 visual magnitude or about as bright as Venus. All observers were in position and ready, starting ≈10 min before expected acquisition and continuing until the news of the crash was heard on the radio.

The reentry was never acquired visually by any of the dozen or so observers at the site. As an afterthought, amber-filtered binoculars would have been useful. The reentry was, however, later found to be recorded on the Mosaic camera tapes from 15:53:33 to 15:53:53 UT. The only events noticed at the time were the audio tone of the forward scatter radar at 15:53:37 UT, somewhat earlier than expected, and a sonic boom at 15:57:11 UT. Nothing was recorded by either the VLF receiver or the more sensitive receivers used by Dr. Martin Beech, University of Regina, Saskatchewan, Canada, in the neighboring campsite. The actual groundtrack is shown in figure 24 of appendix B.

2.1 Initial Video Data Review Notes

Digital video AVI files were made from the original tapes with each file starting ≈15 frames (1/2 s) before the Genesis was visible in the frame using a standard video monitor. File names were of form <Genesis_*n*_obj.avi> where *n* is the camera number. Start universal time for each segment was calculated from a manual synchronizing event—the boxwave, discussed later—and is thus internally consistent to the nearest frame (1/30 s) with an absolute accuracy of ≈0.1 s to GPS (UT) time change. (These notes are not in any particular order.)

(1) The standard video monitors, including the camcorder screen, do not show the digital overscan information delivered by these cameras on the right of the image. The Audio Video Interleave (AVI) frames (720 pixels) are wider by ≈10 percent than the National Television System Committee image. Although each segment began just before the Genesis appeared on the right of the frame displayed using commercial video software (Sony monitor or StudioDV), when viewed full frame using digital video software (Meteor44 or AviSynth), the first frame shows the Genesis already part way across the FOV. This implies lost information. The solution is to remake all the camera AVI files with the same start time. This would simplify comparisons since frame numbers would coincide with the same universal time in each camera and each camera's AVI file would have all useful frames.

(2) In no frame is the Genesis image saturated. As noted below, some of this may be due to lens automatic iris operation, and careful scaling based on background variation (new software) will be required. The partly saturated Moon in camera 3 and the solar glint in camera 2 limited the iris variation due to the Genesis but leaves an uncertainty as to the aperture used. Background stars will be visible during the Stardust reentry and will allow determination of camera variations. Furthermore, the automatic iris feature will be inoperable given the dark sky background.

(3) The modulation of the background due to (presumed) power supply inverter noise is quite visible in false color as vertical stripes in all cameras. It was later determined to be an artifact of the

cameras' color digital signal processing applied to the black and white signal. It is removed by processing using the luminance portion of the signal.

(4) A lens shade is required for all lenses to keep the Sun and sky radiation off the glass. The problem ranges from contrast degradation on cameras 5, 4, and 3 to lens flare in camera 2, and worse in camera 1. An adjustable scrim attached to the Mosaic box—file folder and masking tape—would be a very useful addition for further solar shading.

(5) Camera 5 had the west most field of view and captured the earliest portion of the Genesis reentry observed at Wild Horse with moderate sky background.

- The largest structure in camera 5 is the enhanced atmospheric background at low elevation on the right of the frame. The nominal background on the left is 60 units while on the right it reaches 100 units.

- The Genesis is in the first frame at (286, 134) and has a peak intensity of 89 units. The background is 65 to 70 units.

- The last full frame (115) has the Genesis at (9, 112) with intensity 99 units and background 56 to 60 units.

- Time equation: UT5 = To5 + frame where To5 = 15:53:30:17 (hh:mm:ss:ff); Last Genesis frame (115) = 15:53:34:12 UT.

(6) Camera 4 worked well and captured the Genesis reentry with moderate sky background.

- Genesis appears at (696, 131) with a peak intensity of 150 units and background of 82 to 88 units.

- The largest structure in camera 4 is again the enhanced atmospheric background at low elevation on the right of the frame. The nominal background on the left is 67 units while on the right it reaches 88 units.

- Trail is obvious in frame 88, Genesis coordinates (378, 126) intensity 226 units. Trail extends to (460, 128) and is ≈2 units above the local background of 71 to 76.

- From about frame 60 until the Genesis exits the FOV at frame 157—coordinates (11, 123), peak intensity 136 units—the background oscillates in intensity near the center from 68 to 75 units, which is very visible in false color. It is presumed to be due to the automatic iris operation based on the presence of bright pixels in the image.

- Time equation: UT4 = To4 + frame where To4 = 15:53:33:28 (hh:mm:ss:ff); Last Genesis frame (157) = 15:53:39:05 UT.

(7) Camera 3 contained the Moon as a reference point near the Genesis reentry path.

- Genesis appears at (641, 143) with a peak intensity of 212 units and background of 81 to 85 units.

- The largest structure in camera 3 is the atmospheric scattering with little polarization at the upper left of the frame. The nominal background at the upper left is 105 to 110 units while on the right it is about 74 to 83 units.

- Trail is weak from the start and is gone by frame 30; Genesis coordinates (460, 149) with intensity of 221 units. Trail is very short and is <2 units above the local background.

- The Moon is in the FOV at (289, 212) and is partially saturated (255 units). The closest pass to the Moon is frame 56 at 15:53:40:26 UT. The Genesis exits the FOV at (9, 166) with intensity 158 units.

- The background is steady until the Genesis exits the FOV, at which point it becomes slightly unstable. This presumably has something to do with the automatic aperture.

- Time equation: UT3 = To3 + frame where To3 = 15:53:39:00 (hh:mm:ss:ff); Last Genesis frame (99) = 15:53:42:09 UT.

(8) Camera 2 had a bad Sun glint but a portion of the reentry was observable.

- Genesis appears at (471, 192) with a peak intensity of 92 units and background of 68 to 75 units. The clip should have started much sooner.

- The brightest structure in camera 2 is the solar lens flare at the lower right of the frame. The largest structure in camera 2 is the atmospheric scattering with little polarization at the upper left of the frame. This leaves a darker background band from upper right to the bottom center. The nominal background at the upper left is 97 to 102 units, lower right reaches 210 units at (687, 22), while at the upper right there is a dark patch of about 55 to 60 units. A lens shade and/or a scrim would have been very useful since the Sun was not close to the FOV.

- Genesis fades into the background in frame 87 at (291, 207) with peak intensity 82 units and background 72 to 81 units at 15:53:56:08 UT.

- Time equation: UT32 = To2 + frame where To2 = 15:53:43:11 (hh:mm:ss:ff); Last Genesis frame (87) = 15:53:56:08 UT.

(9) Camera 1: No data. Camera 1 was capped since it had the full glare of the Sun on its glass. A lens shade and/or a scrim would have been very useful since the Sun was not actually in the FOV. In any case, the Genesis was fading significantly by this time and might not have been visible in camera 1.

(10) Camera 10 was a Sony Handycam and was time synchronized with the other cameras. Although no useful images were obtained, the camera recorded a sonic boom on the audio track at 15:57:11 UT and the tone from the forward scatter radar at 15:53:37 UT as well.

2.2 Mosaic Camera Photometry

To facilitate the preparation of a precise photometric timeline spanning the four cameras used, new AVI files were prepared, all starting at precisely 15:53:30 UT and designated <Genesis_0*n*.avi> where *n* is the camera number. Flatfields were prepared for each camera lens combination and used for lens falloff compensation (small). Standard video calibration techniques were used to determine each camera's gamma (significant), and this gamma was used in all photometry. Appropriate avicubes were made and the capsule was tracked automatically for camera 4 and manually for the other cameras as required. Circular aperture photometry was performed with appropriate apertures and an extreme variation (flicker) was observed (app. B) that had nothing to do with the apertures used. The extreme flicker complicated the automatic tracking, causing the object to be "lost" when it was extremely dim. The overlap between the cameras was used to scale one camera to the next and the conjunction with the last quarter Moon provided a precise time and intensity calibration. See figure 6.

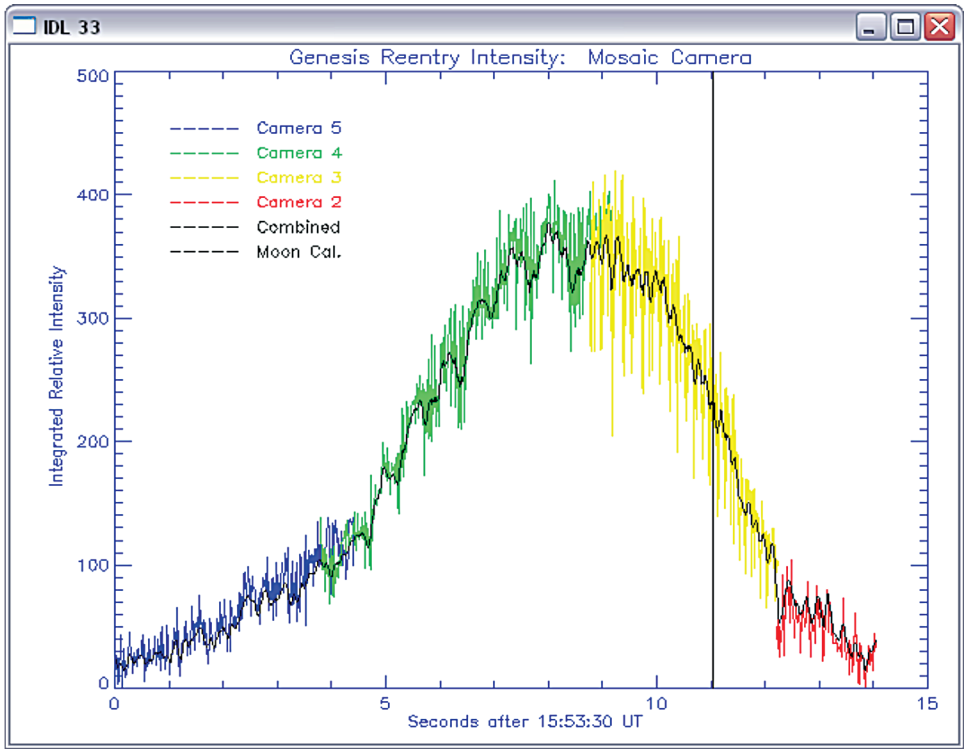

Figure 6. Combined photometric intensity in instrument units. The overlap between cameras has been used to adjust the gain of cameras 2, 4, and 5 to that of camera 3. The Genesis intensity and timing at lunar conjunction (vertical line) as seen by camera 3 is used for time and intensity calibrations. Camera 2 included a significant Sun glint which limited detectability.

Although these data have been smoothed, the residual flickering is real and is often observed on reentry—discussed further below. The relatively smooth central portion coincides with the observation of a definite trail. The trail and flickering seem to be mutually exclusive. If the emission is primarily air excitation similar to this arcjet spectrum, then the visual magnitude is the instrument magnitude plus 2.29 for a peak visual magnitude of –5.4 (fig. 7). If the spectrum is more like a 2700K blackbody, then the color index is –1.97 for a peak visual magnitude of –5.7. Spectral concerns and how they affect the observations and calibrations are discussed further in appendix A.

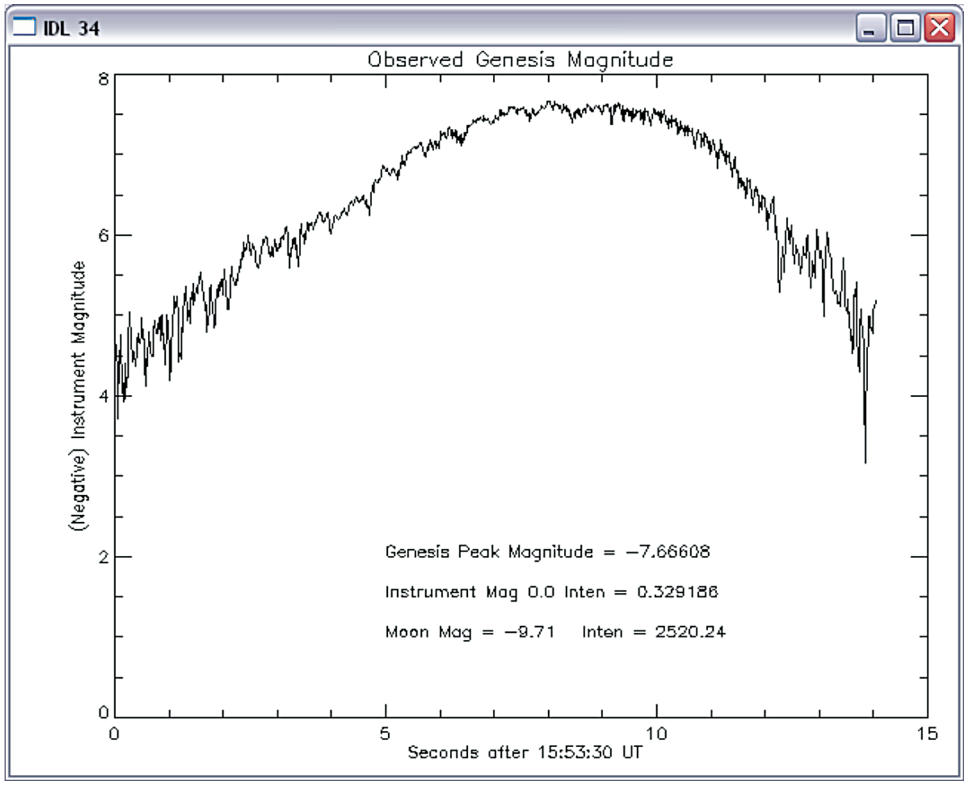

Figure 7. Observed instrument magnitude: Reference last quarter Moon at –9.10 visual magnitude with instrument color index of –0.61. Visual magnitude is estimated as 2.29 magnitude dimmer than above.

A revised trajectory and timeline was obtained courtesy of Prasun Desai, NASA Langley Research Center, based on their postflight analysis (app. C). The conjunction of the Genesis reentry with the Moon as observed from the observing site was used to find the entry interface (EI) in terms of UT and thus affix the trajectory timeline. Determination of the time of EI was within the expected bounds. Figure 8 shows the resulting timeline.

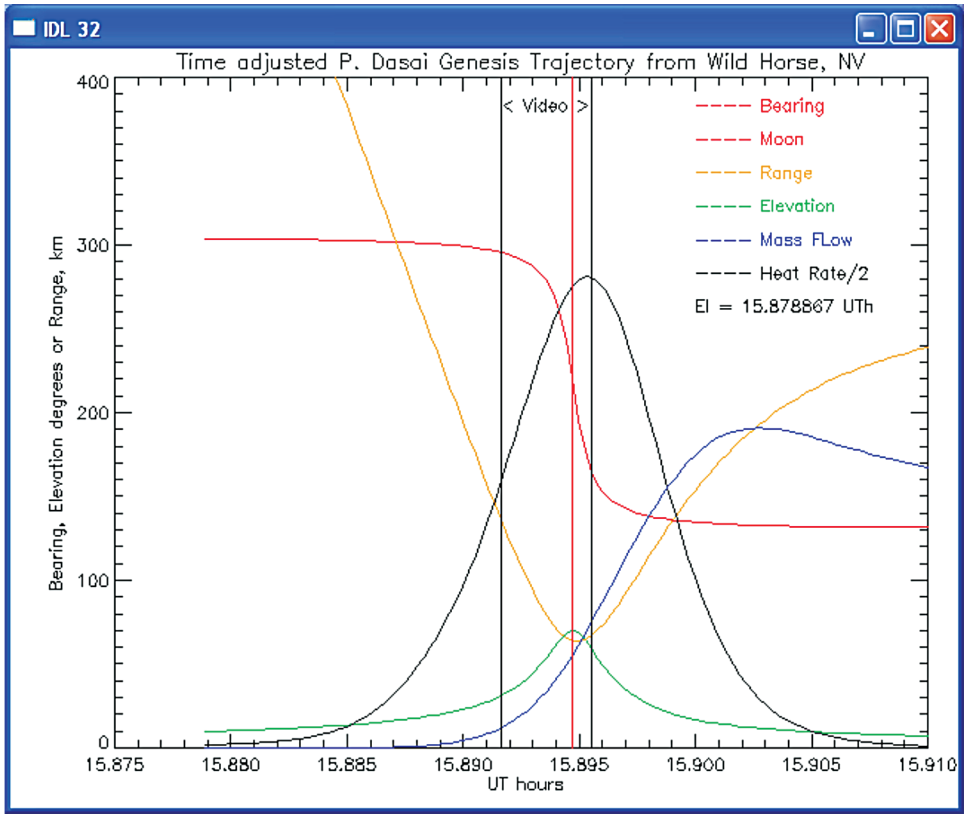

Figure 8. Genesis postreentry trajectory as determined by P. Dasai and viewed from Wild Horse, NV. The bearing and time of the lunar conjunction (vertical red) was used to find the time of EI (15:52:43.9 UT) and to align with the video images.

Atmospheric effects were modeled using DayStar44 with ModTran for mid-summer continental dry conditions at multiple wavelengths. One output—the optical transmissivity from the site at 2 km altitude to space—shown in table 1, was used to find the optical depth at that wavelength. This optical depth was used with the slant path range to determine the atmospheric correction. The slant range was also used to correct the intensity to a constant 100-km effective range using the inverse square law. The results are shown in figure 9.

Table 1. ModTran modeled atmospheric transmissivity over Wild Horse, NV.

Wavelength (nm)	Zenith (18 km)	Minimum Range (65 km)	Reference (100 km)	Maximum Range (130 km)	Optical Depth (km)
625	0.85851	0.577	0.429	0.332	118
714	0.88672	0.648	0.513	0.42	149.7
750	0.90677	0.702	0.581	0.493	183.9
833	0.85201	0.561	0.411	0.315	112.4
909	0.68191	0.251	0.119	0.063	47

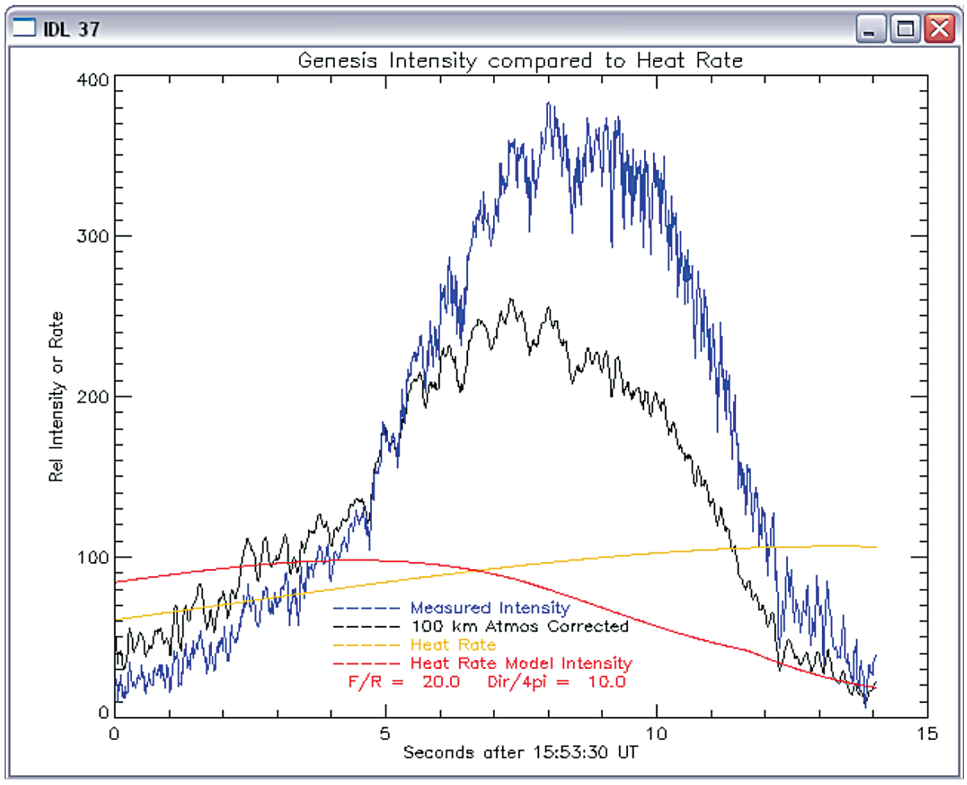

Figure 9. The P. Dasai postreentry trajectory as viewed from Wild Horse, NV, was used to correct the instrument intensity to 100 km standard distance and for atmospheric extension over the slant path range.

The atmosphere corrected, 100-km intensity is shown in figure 9. Two very simple models of the emissions are also shown. The simplest model assumes that the emissions are emitted equally in all directions and vary directly with the heat rate. Note that the heat rate peaks at 15:53:44 UT at the right in figure 9. If the observed emission was predominately based on the rate of energy lost by atmospheric deceleration, then the light curve would parallel the "heat rate" curve. Since the light curve is not even close to being parallel to the heat rate, the emissions are obviously more complex. The second simple model is based on the spacecraft geometry and site view angles as a modulation of the heat rate. This heat rate/geometric model is labeled "heat rate model intensity" in figure 9.

The heat rate/geometric model assumes a double conical spacecraft with Genesis' dimensions (app. D) moving with the cone axes along the flight path. The portion of light emitted directly from the cone surfaces is proportional to the projected area of the surface as seen from the site at an angle from the flight path α. As the craft approaches the site, it first presents the hot front surface; and as it continues past the front, it is shaded by the cooler rear of the craft. The craft is assumed to emit light proportional to the heat rate, with an adjustable fraction emitted from the projected area of the front cone, the projected area of the rear cone, and spherically to all of space. The "heat rate model intensity" shown in figure 9 assumes that only 10 percent is radiated evenly into all space (4π) and that the rear component is only 5 percent of the remainder so that the modeled intensity is very view angle dependent. Although this reproduces the asymmetry seen in the atmospheric corrected intensity, the bright hump from 5 to 12 s is not predicted at all.

Since the fidelity of this heat rate/geometric model is low, the primary lesson is that something besides geometry and heat rate is required to explain the observations. The large, bright hump in excess of the model from 5 to 12 s is perhaps due to ablation emissions, which are not in this geometric model. In this time period, the Genesis speed varies little from 10 km/s and ranged in altitude from 68 to 61 km. The air density ranged from 1×10^{-4} to 2.5×10^{-4} kg/m^3. This rather short altitude range falls near the expected height of appearance for slow (10 km/s) fireballs. The peak of this optical emission occurs 7 s before peak heating (14 s) and roughly corresponds to the observed trail. The trail is observable from 5.6 to 9 s after 15:53:30 UT with a peak at ≈7 s as shown in figure 10.

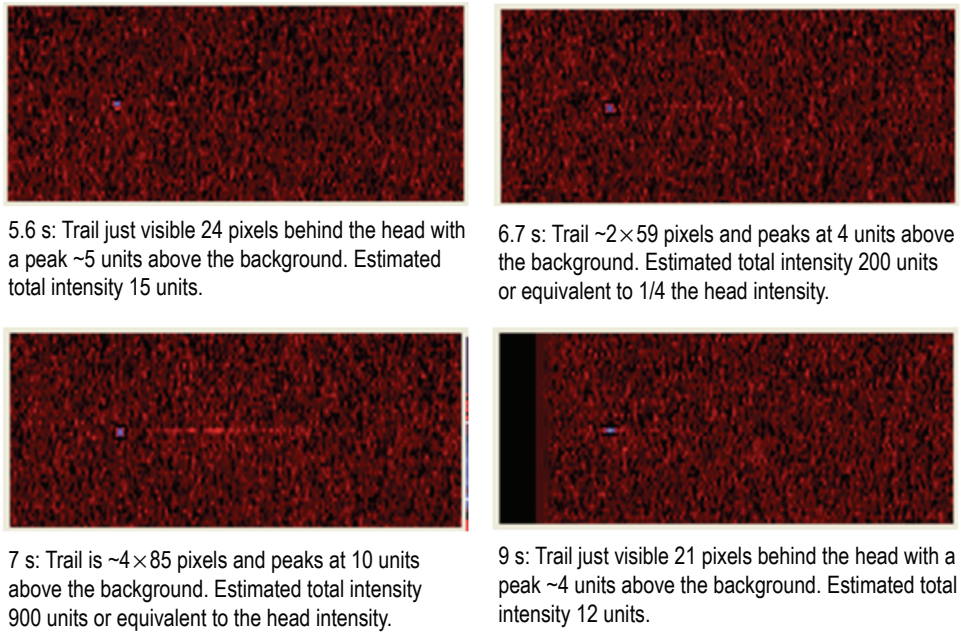

5.6 s: Trail just visible 24 pixels behind the head with a peak ~5 units above the background. Estimated total intensity 15 units.

6.7 s: Trail ~2×59 pixels and peaks at 4 units above the background. Estimated total intensity 200 units or equivalent to 1/4 the head intensity.

7 s: Trail is ~4×85 pixels and peaks at 10 units above the background. Estimated total intensity 900 units or equivalent to the head intensity.

9 s: Trail just visible 21 pixels behind the head with a peak ~4 units above the background. Estimated total intensity 12 units.

Figure 10. Trail observed following the Genesis as viewed in false color by camera 4.

2.3 Mosaic Camera Photometry Summary

This experiment demonstrated that a simple array of commercial video cameras can photometrically record reentry emissions even under daylight conditions. A stationary, staring array reliably captured data even though the reentry was never seen visually. As expected, the brightest emissions are shown to be largely due to ablation. These data provide valuable constraints on meteor and reentry models. Similar techniques are even more productive during nighttime reentries with their dark sky.

3. FORWARD SCATTER RADAR OBSERVATIONS OF GENESIS SPACECRAFT ENTRY

A radio receiver was deployed at the Wild Horse Reservoir site to test the utility of a forward scatter radar system. MSFC has extensive experience with this technique in the detection of meteors. Space Shuttle *Columbia* was observed using this technique during STS–107 by an amateur radio meteor observer in New Mexico. This technique consists of tuning a radio receiver to the video carrier frequency of a distant TV station and recording the receiver audio output. Since the TV signal is at very high frequencies (VHFs) that can only propagate by line of sight—no signal is detected until a meteor or a spacecraft enters the atmosphere and generates plasma of sufficient density to reflect the signal. The plasma generated by the Genesis spacecraft was clearly detected and the Doppler shift caused by the spacecraft motion was detected along the scattering paths to two different TV transmitters. The Doppler profiles closely match those computed for the Spokane, WA, and Klamath Falls, OR, transmitters as shown in figure 11.

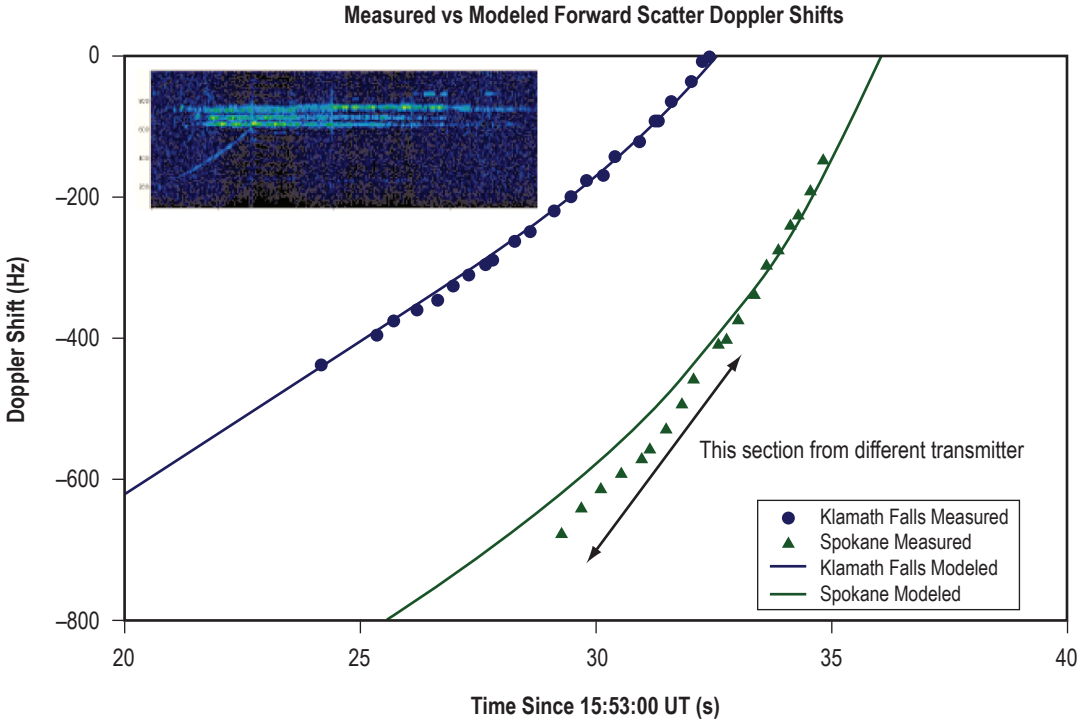

Figure 11. Spectrogram of radio receiver output (inset) compared to Doppler profile modeled using predicted Genesis trajectory. The blue line is for Klamath Falls, OR, and the green line is for Spokane, WA.

3.1 Forward Scatter Radar Observations

Note that the receiver passband is inverted by the continuous wave (CW) product detector in the receiver so the Genesis "head echo" appears to move from lower to higher frequency (velocity) relative to the transmitter/receiver pair. The horizontal bars in the lower part of figure 11 are the ionization trail which is left in the atmosphere and is not moving significantly relative to the transmitter/receiver.

The Doppler shift of the received signal is computed from

$$F = 1/\lambda * (dR_T/dt + dR_R/dt) \quad , \tag{1}$$

where λ is the wavelength of the transmitter signal (5.4308 m for frequency of 55.24 MHz), and dR_T/dt and dR_R/dt are the range rates between the spacecraft and the transmitter and receiver, respectively. The predicted trajectory was used with the Satellite Tool Kit to compute the range rate as a function of time. In order for the Doppler shift to pass through zero frequency and hence fall within the 2-kHz passband of the receiver, the sum of the range rates must be small, which occurs when the spacecraft is moving away from one at the same rate as it is moving toward the other. This condition only occurred for the Spokane and Klamath Falls transmitters (fig. 12).

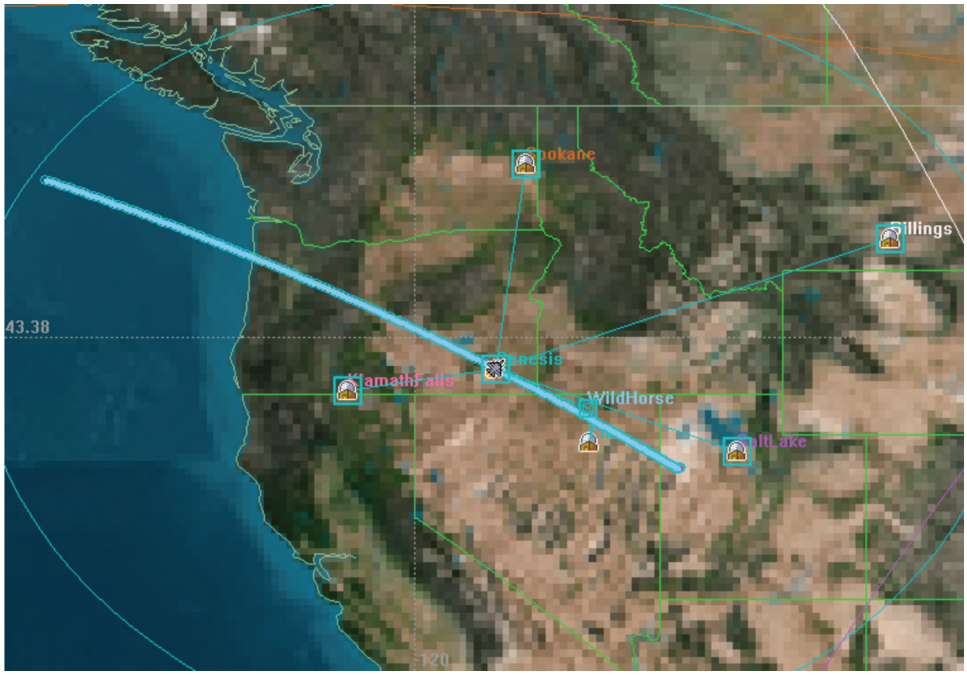

Figure 12. Geometry of the Genesis trajectory and TV transmitters at the receiver frequency of 55.24 MHz, TV channel 2, with negative carrier offset as computed by Satellite Tool Kit.

The receiver used was an Icom PCR–1000 computer-controlled unit (fig. 13). Any receiver capable of performing CW or single-sideband detection at frequencies in the VHF television band will work. A database of TV transmitters in the United States, Canada, and Mexico was downloaded from

the Federal Communications Commission (FCC) Web site. The frequency was selected by tuning the receiver through the possible carrier frequencies in the lower VHF band until a relatively quiet frequency was found; i.e., there were no close-by transmitters, but meteor echoes were detectable, indicating that there were some transmitters at the proper range to illuminate the sky above the observing site. The FCC database was used to identify stations in the proper frequency range. The antenna was a simple "rabbit ear" dipole attached to the top of a van. The audio signal from the receiver was fed into the sound card of a laptop computer, digitized, and saved to hard disk. A fast Fourier transform (FFT) sound analysis program, SpectraPro, was used to compute and view the spectrogram of the signal.

Figure 13. Laptop computer and PCR–1000 receiver (on shelf on the right) used to collect forward scatter radar data. A VLF receiver is visible at lower left.

The output of a VLF receiver with a large loop antenna was also recorded during the entry but no signals were obvious.

3.2 Forward Scatter Radar Summary

This experiment demonstrated that a simple forward scatter radar system utilizing TV transmitters as the illumination source could detect the ionization trail left by the Genesis spacecraft as well as the ionization around the spacecraft itself—the "head echo" in meteor radar parlance. This head echo produced observable Doppler shifts that matched those modeled for the predicted entry trajectory. It is possible that a similar technique could be employed during the space shuttle and other spacecraft entries to provide some information about the plasma conditions of the entry and, with sufficient dynamic range, possibly detect objects that might detach from the entering vehicle.

4. LESSONS LEARNED

The following lessons learned—in no particular order—were immediately evident soon after the observations:

- A stationary, preaimed camera array like the Mosaic array is a valuable backup to more sophisticated tracking instruments. Much can be learned from simple photometry and timing.

- Do not trust other people's magnitude calculations. The initial estimations based on simple meteor theory with small ablation were closer than some researchers' predictions and could have prevented some of the problems due to the emissions being fainter than expected.

- Start out pointing the Tracker array at a precalculated position until visual acquisition and tracking is possible.

- Sunshades or scrims are required when observing in the daytime to keep the Sun off the lenses and filters to avoid Sun glints.

- There were problems imaging the GPS receiver display with the cameras to record time. An improved method of time recording from GPS is needed.

- A very bright monitor properly oriented is needed in the daylight.

- Binoculars with red or amber filters are needed for visual acquisition in the daylight.

- The ability to generate star field maps with trajectory overlays is needed in the field for trajectory updates when site changes are necessary.

- Better communication is needed. There was no cell phone coverage, and a data link would have been a great asset, particularly for shuttle reentries where real-time updates may be necessary.

- High gain VLF antennas are needed for what appears to be, at best, weak signals.

- Equipment is transported much better using a large SUV as opposed to a car or minivan. A camper would allow more site flexibility and comfort.

- A fourth person with a checklist would be useful to double-check recorders, sunshades, power, focus, camera settings, timing, etc. The team had three people.

- Bring a large photo flash and appropriate white card to synchronize all cameras.

- Although spectra of the reentry are extremely useful for calibration and analysis, much can be done using simple assumptions about the spectral character of the emissions.

The following were noted in personal communication with Prasun Desai concerning postflight trajectory analysis using tracking radars:

- Improved timeline communication and clock synchronization between mission operations and the observing radar units.

- Multiple radar locations to improve the accuracy of the postflight trajectory.

5. IMPLICATIONS FOR STARDUST OR SHUTTLE REENTRY OBSERVATIONS

The implications for ground-based Stardust and shuttle reentry observations are clear. Much can be learned from simple ground-based photometric video observations, even in broad daylight. Even more can be determined when the photometry is supplemented with spectroscopy. Even low-resolution spectral information is useful for determining the different phases of the reentry, temperatures, ablation rates, and color indices for comparison to traditional meteor analysis.

Stardust will reenter at about 3:00 a.m. local civil time (MST) on January 15, 2006, with a full Moon high in the sky. Although smaller than Genesis at 45.8 kg and an 81.1 cm diameter, it will reenter at a faster 12.9 km/s and ablate its thick phenolic-carbon heat shield at a greater rate. Peak brightness should be very similar to that of Genesis. This should make acquisition reasonably easy, even with the full Moon. Filters and polarizers will not be needed. The capsule brightness will require careful camera adjustment in order to keep the saturation of the capsule in the calibrated range while still imaging enough of the brighter stars to facilitate tracking and intensity calibration.

One of the advantages of a bright nighttime reentry and its dim sky background is that all of the cameras in the Mosaic array can be fitted with transmission gratings so that a continuous low-resolution spectrum will be recorded along with the zero-order photometry and timing. The low-resolution spectra thus obtained will be able to discern the fraction of blackbody and plasma radiation and will show the bright sodium lines characteristic of heat shield ablation. This fixed-camera array has proven itself to be an extremely reliable performer.

The Tracker array will supplement the Mosaic array and, assuming accurate prior knowledge of the reentry trajectory, should provide excellent photometry and low-resolution spectrometry for both earlier and later portions of the reentry. Again, camera adjustment will need to be carefully done to capture calibration stars while keeping the intensity of the capsule within calibrated intensity range.

Shuttle reentries are most likely to approach from the south. This places severe constraints on observing site selection—either water or Mexico. The northerly approach over the United States works much better for ground-based observations. Lessons learned (sec. 4) from the Genesis reentry apply directly here to daylight shuttle reentries. Normal shuttle reentries are nonablative so the brightness should be similar to Genesis even though the size and energy is greater. Continuous communication of the latest expected trajectory and any updates or delays will be critical. As currently organized, changing the viewing site will require at least 2 hr plus travel time or three orbits notice. Either multiple ground stations chosen to cover alternate ground tracks or airlift capability would be needed to assure data collection.

APPENDIX A—SPECTRAL CONSIDERATIONS

The images are comprised of sky background, the Moon, and the target, each with its characteristic spectrum. They are recorded with a camera with a unique spectral response modified by a strong red filter. The goal here is to model these responses in order to predict visibility, make comparisons for calibration purposes, and interpret the results in traditional visual magnitude terms. The following calculations and plots (figs. 14 and 15) were produced using DayStar44 with ModTran4 and a catalog of filter, detector, and target spectra.

Color indices were calculated for lunar, arcjet, and 3700K blackbody emissions using standard astronomical ultraviolet, blue, visual, red, infrared (UBVRI) filters and the filtered instrument by comparing each emission's response through each filter or the filtered instrument in turn with the same response to a precision Vega model. Vega is the astronomer's standard candle and is defined to have a magnitude of zero in every band or as viewed with any instrument. The results are shown for the three emissions in figures 16–18. The UVBRI indices are the result of comparing the emission and Vega as viewed through the appropriate color filter with a perfect detector. Similarly, the filter/camera combination is used to compare the emission and Vega to get the "Inst_ndx" shown in the plot.

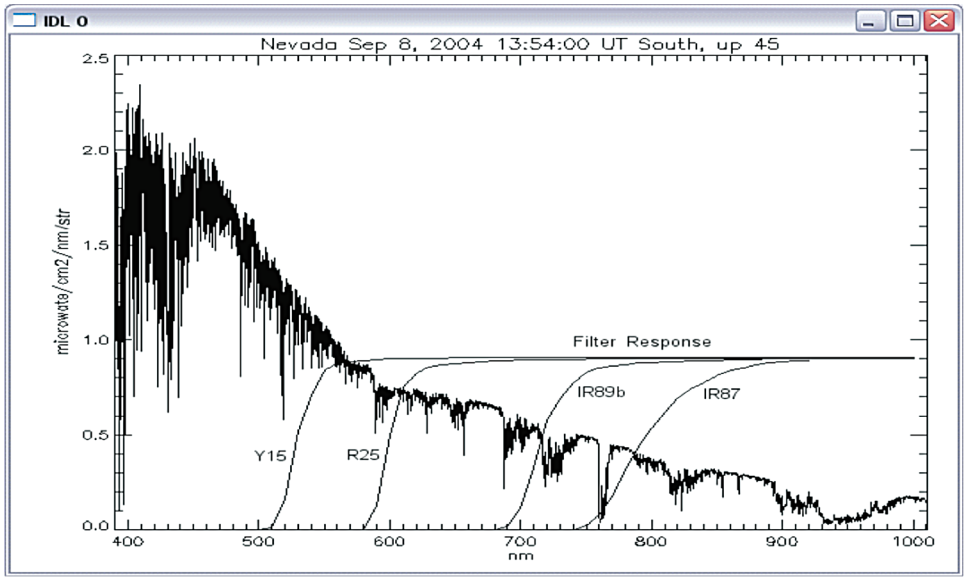

Figure 14. The effect of filtration using various common filters (Y15, R25, IR89b, and IR87) on morning scattered solar and lunar radiation in northern Nevada. Filter R25 with a linear polarizer was chosen.

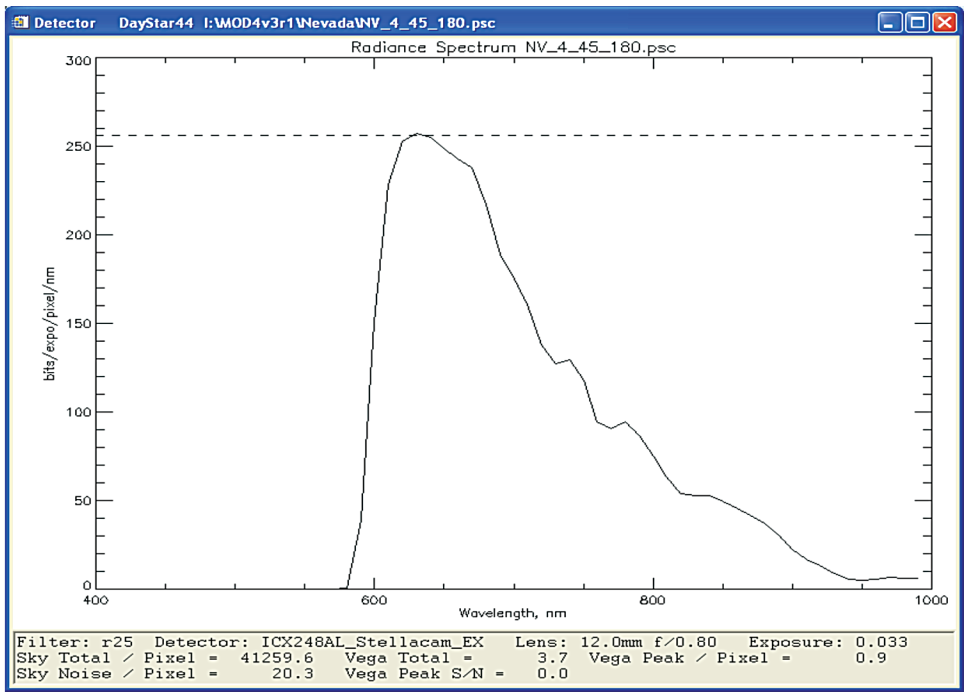

Figure 15. Sky response with our StellacamEX cameras fitted with a 12mm, f/0.8 lens and R25 filters.

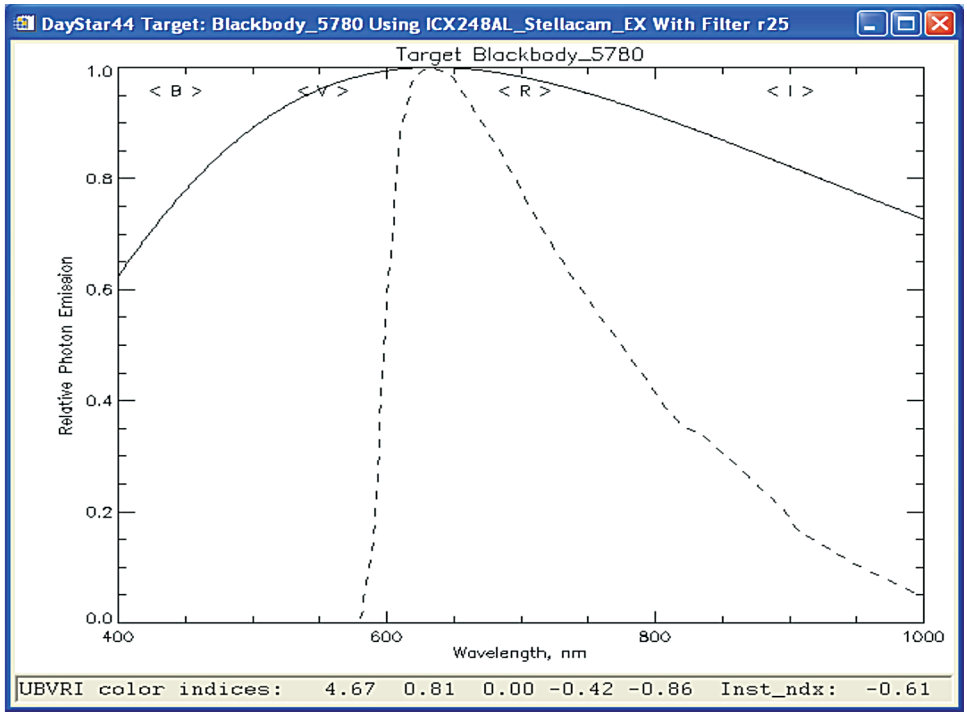

Figure 16. Simulated solar/lunar spectrum (solid) and simulated response (dashed) with StellacamEX and R25 filter.

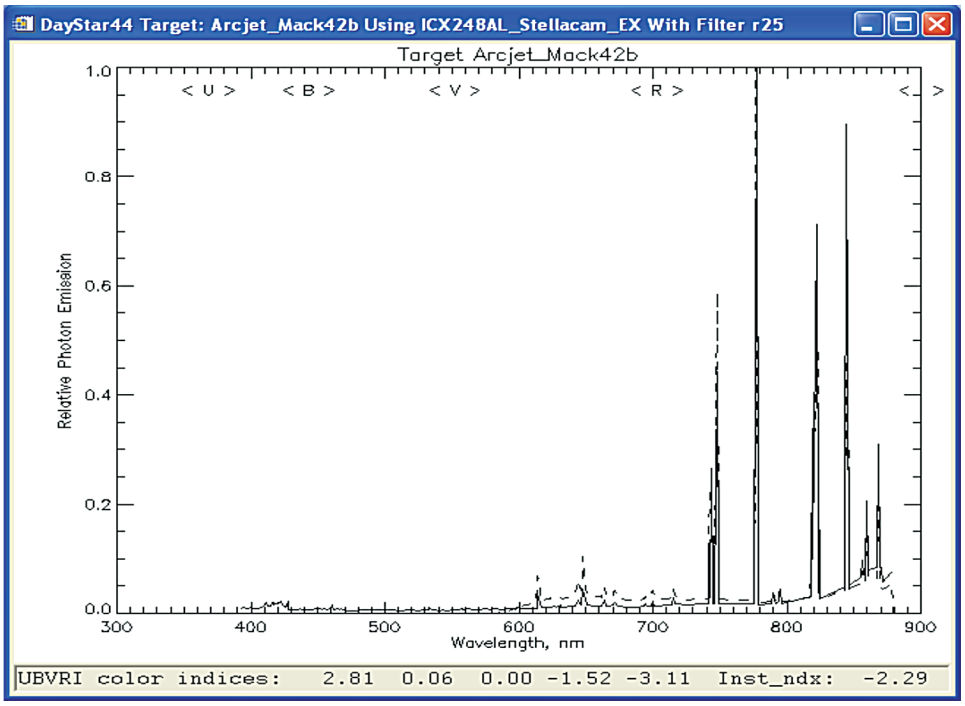

Figure 17. Arcjet plasma spectrum (solid) and simulated response (dashed) with StellacamEX and R25 filter.

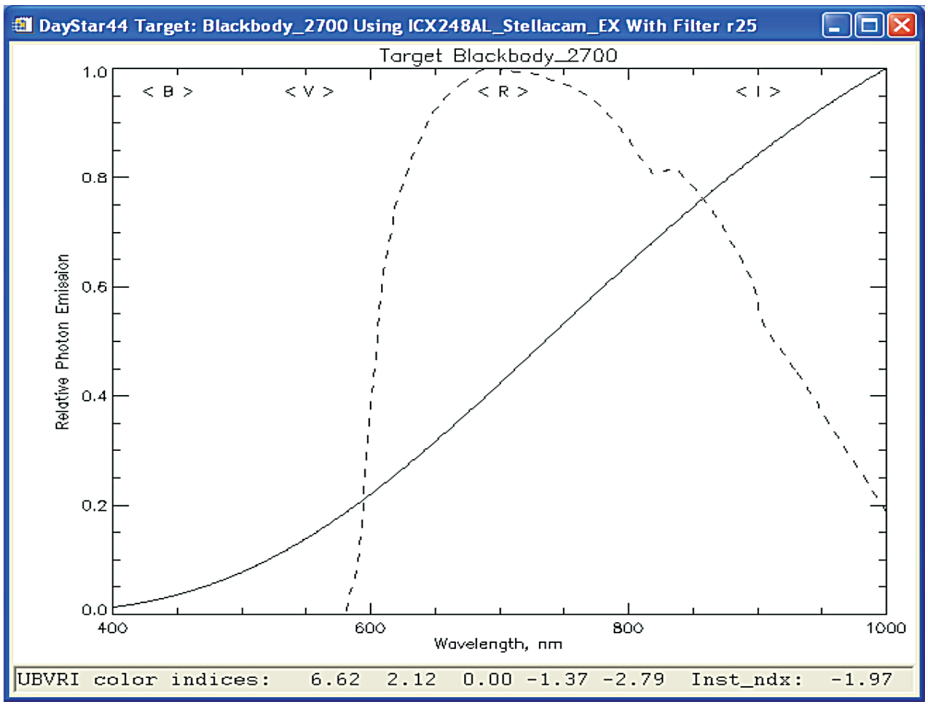

Figure 18. 2700K blackbody (solid) and simulated response (dashed) with StellacamEX and R25 filter.

The appropriate color index is used to estimate the visual magnitude of an emission given its magnitude in one of the other bands. Conversely, it can be used to estimate the instrument magnitude of a known emission given its visual magnitude. For example, the instrument color index for a 5780K (lunar/solar approximation) blackbody of –0.61 implies that the Moon in the observations with a calculated visual magnitude of –9.10 has a lunar instrument magnitude of –9.71. This known instrument magnitude is then used to calibrate the instrument magnitude of the Genesis in the same scene. The Genesis instrument magnitude can be converted to equivalent visual magnitude using either the arcjet spectrum or the 2700K blackbody in the absence of an actual reentry spectrum.

Using the arcjet spectrum, a visual magnitude of zero implies an instrument magnitude of –2.29 due to the strong near-infrared lines. If the emission is primarily air excitation similar to the arcjet spectrum in figure 17, then the visual magnitude is the instrument magnitude plus 2.29, so that a peak instrument magnitude of –7.7 implies a peak visual magnitude of –5.2. If the spectrum is more like a 2700K blackbody as in figure 18, then the instrument color index of –1.97 implies a peak visual magnitude of –5.5. There is only a difference of 0.3 in visual magnitude between these rather different, but perhaps reasonable, reentry spectra.

APPENDIX B—FLICKER

The observed intensity of the reentry flickers widely over a small time period. This is consistent with observations from the cabin of the space shuttle which shows intense bursts of light at the beginning of reentry followed by a bright plume with even brighter fire balls erupting at rapid, irregular intervals. The raw data from these observations often seem to disappear into the sky background only to quickly flare brightly. In order to eliminate camera effects, the raw data from the overlap periods were plotted in figures 19–21. The data are field by field so each "point" is the integral over the period from the point before to the point after. Only slight shifts, well within the relative time synchronization accuracy of two fields, produce significant correlation consistent with the flicker being an effect of the observation and not the cameras.

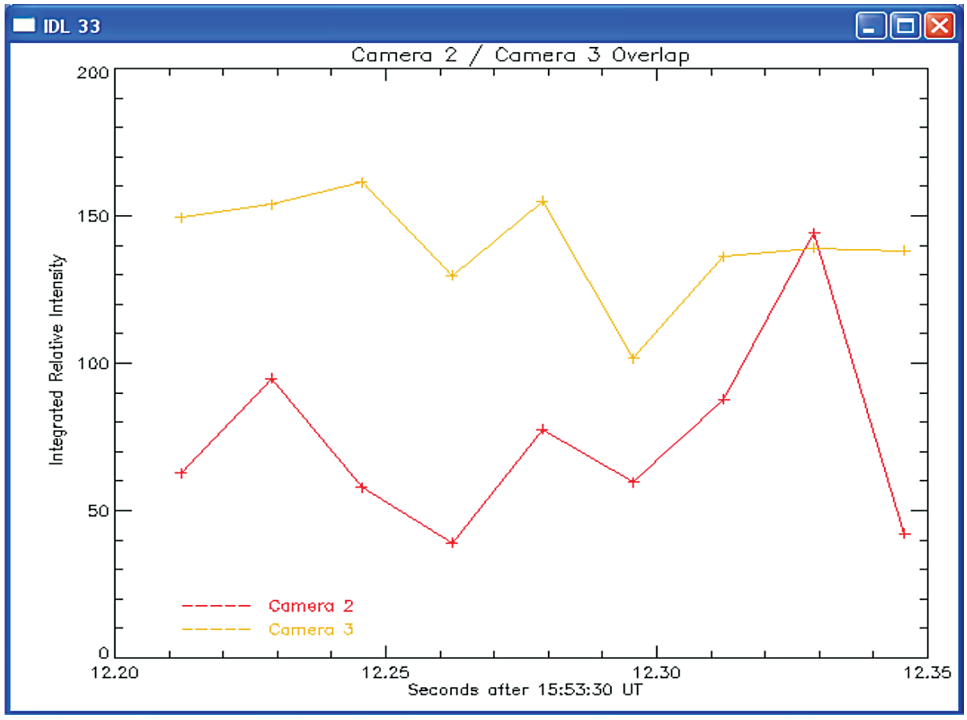

Figure 19. Cameras 2 and 3 are partially synchronized over this short period of overlap.

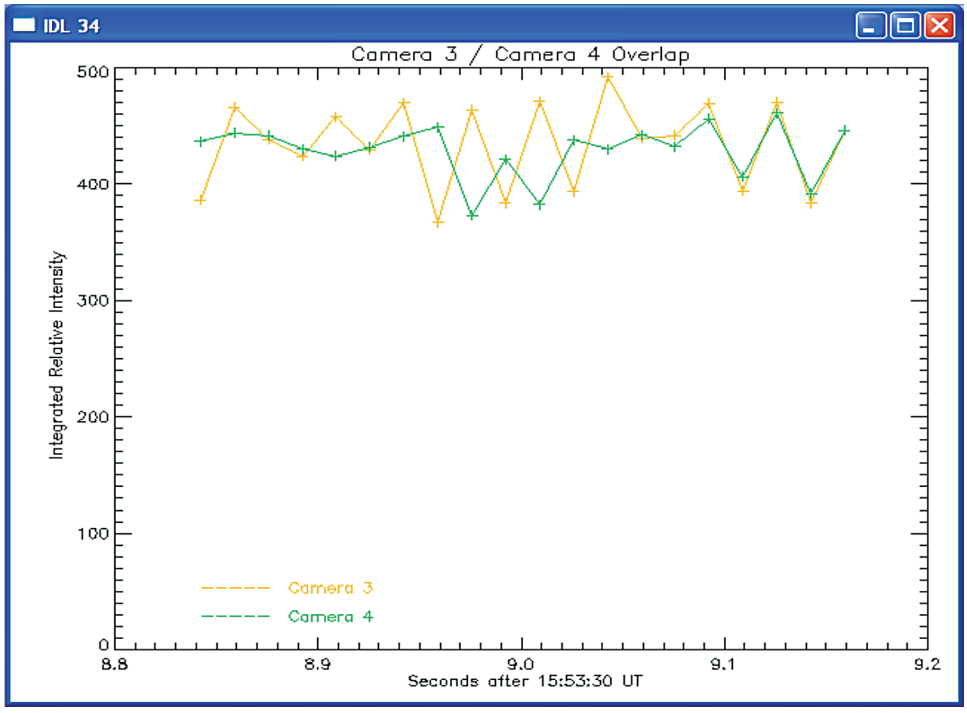

Figure 20. Cameras 3 and 4 are within one-half field of being synchronized.

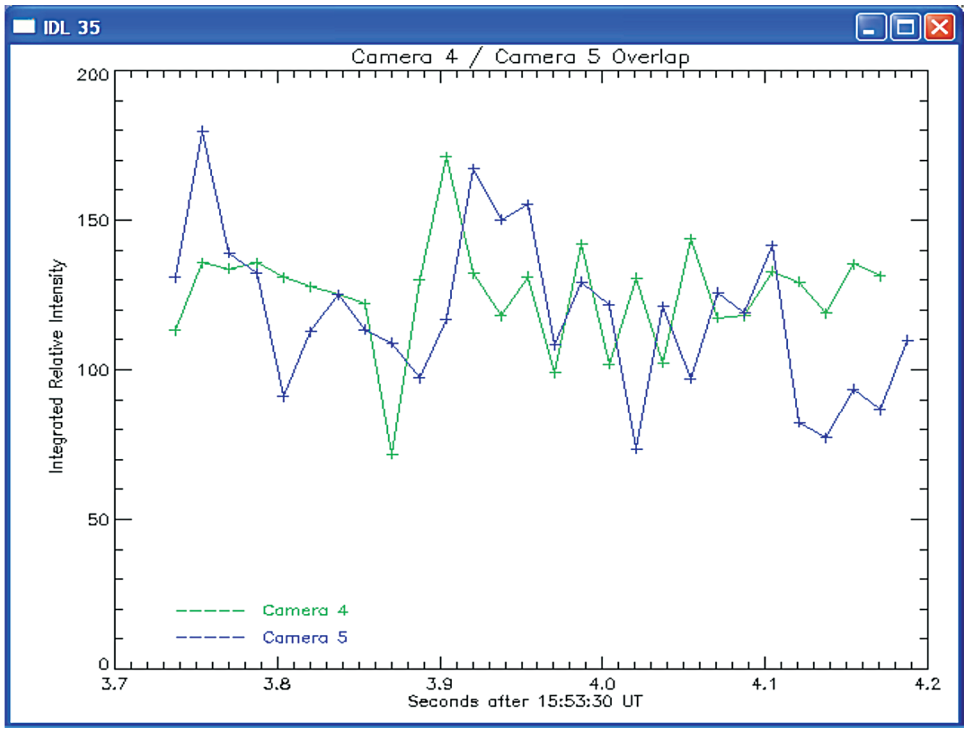

Figure 21. Shifting camera 4 data one field to the right produces a significant correlation.

Visual examination of the time series of intensity (fig. 6) seems to yield periodicities in the flicker. To more closely examine the data for such effects, the discrete Fourier transforms (DFTs) of the data from each camera were plotted in figure 22. No characteristic peaks were found. Flat white noise predominates with a significant 1/F flicker at extreme low frequencies. Excess noise at approximately 5 Hz in cameras 5 and 3, at 27 Hz in camera 3, and at 12 Hz in camera 2 may not be significant but can be picked out in the time plots. Nothing seems to correlate to any significant extent in the combined plot. The current hypothesis is that the flicker is atmospheric in origin.

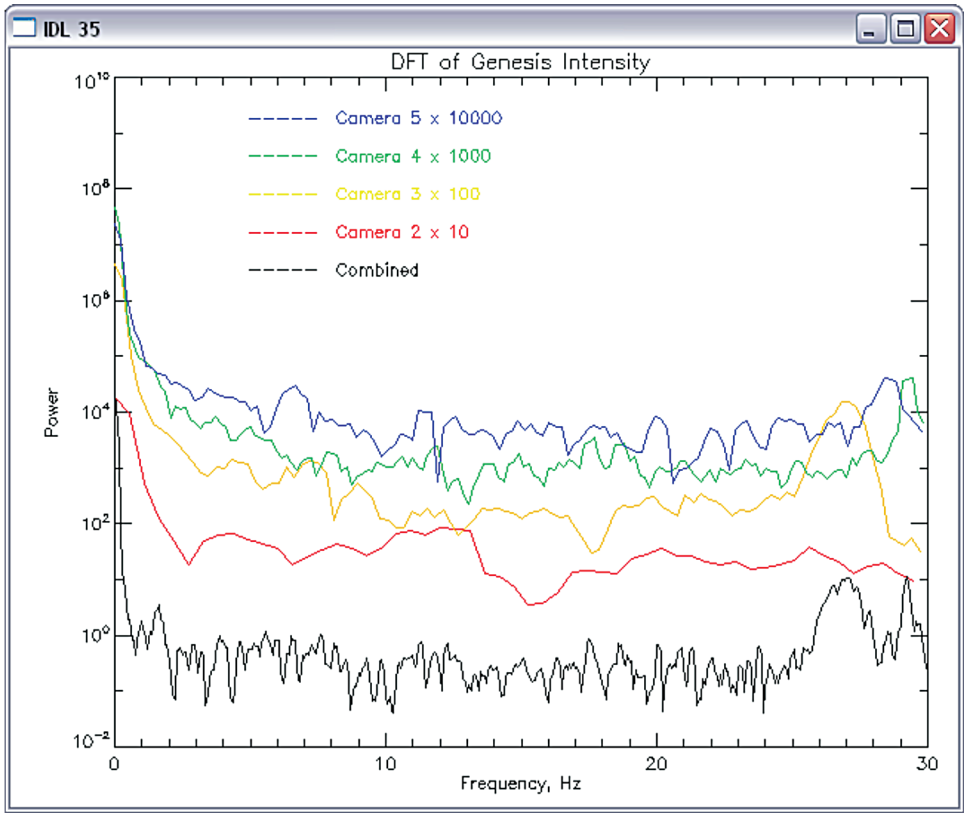

Figure 22. Frequency analysis (DFT) of each camera and the combined record. The main features evident in these plots are the white noise and flicker (1/F) noise.

APPENDIX C—GENESIS GROUND TRACK MAP

Figure 23 shows the ground track map of Genesis.

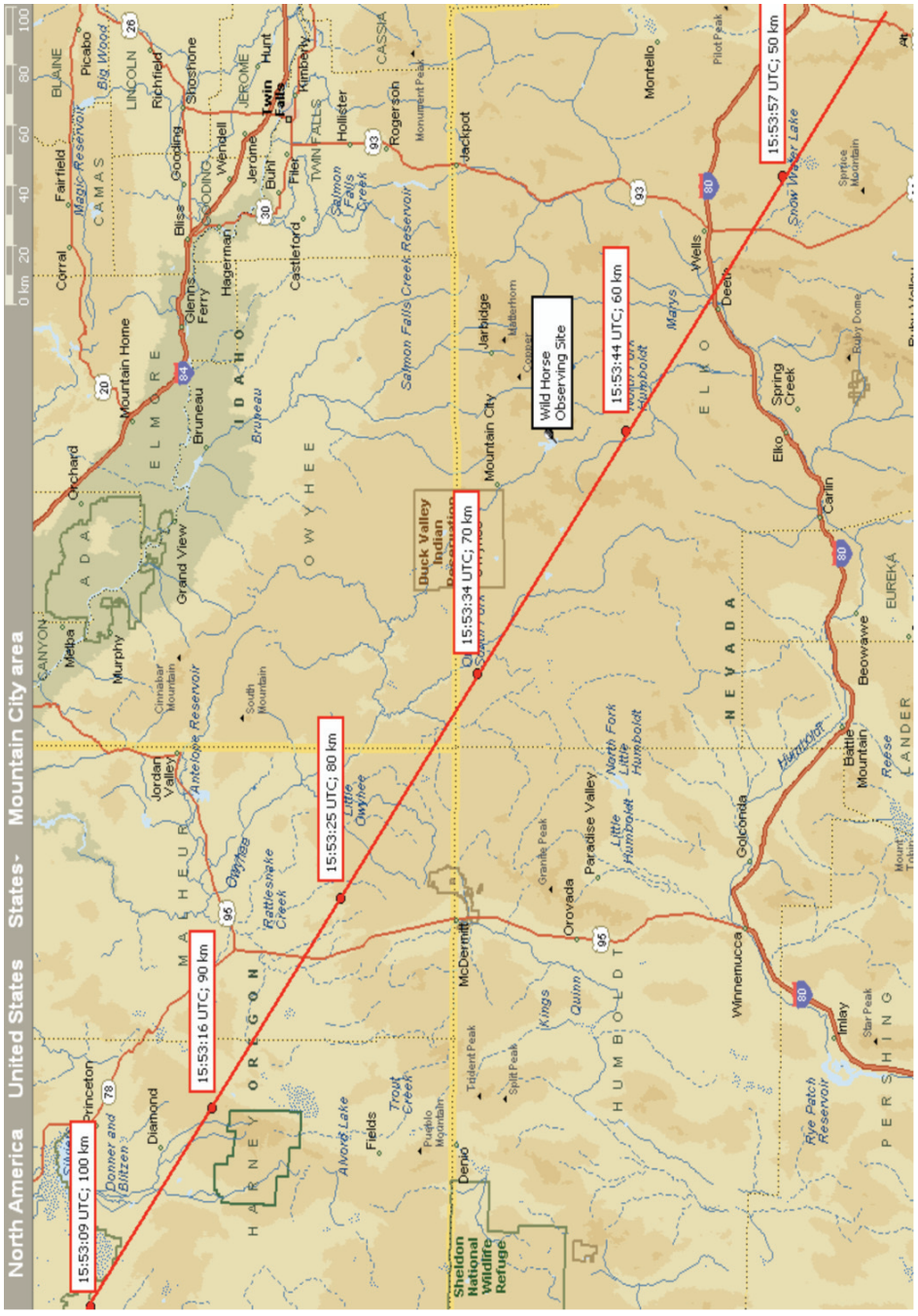

Figure 23. Genesis ground track map.

APPENDIX D—SAMPLE RETURN CAPSULE DESCRIPTION

The sample return capsule (fig. 24) details are as follows:

- Diameter: 1.52 m (60 in)
- Height: 0.81 m (31.7 in)
- Mass: 225 kg
- Speed: 11 km/s
- Entry angle: 8º
- Spin rate: 15/s
- Expected peak brightness: –9.2 magnitude (360–630 nm, at 100 km distance)
- Landing site: U.S. Air Force Utah Test and Training Range
- Heat-shield material: Carbon-carbon (nonablative)
- Rear heat shield material: SLA–561V (lightweight ablator)
- Peak heating: 750 W/cm^2.

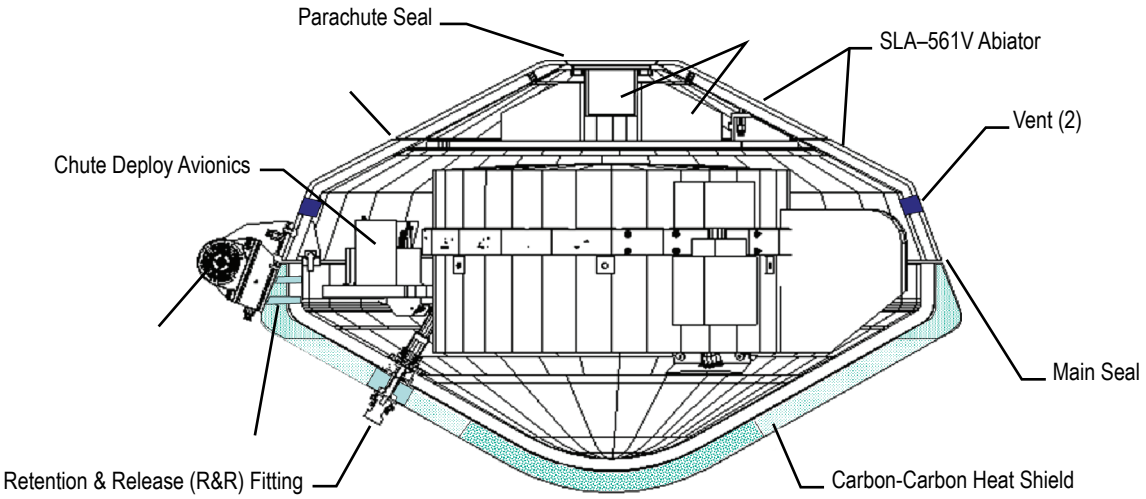

Figure 24. Sample return capsule.

REPORT DOCUMENTATION PAGE

Form Approved
OMB No. 0704-0188

1. AGENCY USE ONLY *(Leave Blank)*	2. REPORT DATE	3. REPORT TYPE AND DATES COVERED
	November 2005	Technical Memorandum

4. TITLE AND SUBTITLE

Genesis Reentry Observations and Data Analysis

5. FUNDING NUMBERS

6. AUTHORS

W.R. Swift* and R.M. Suggs

7. PERFORMING ORGANIZATION NAME(S) AND ADDRESS(ES)

George C. Marshall Space Flight Center
Marshall Space Flight Center, AL 35812

8. PERFORMING ORGANIZATION REPORT NUMBER

M–1154

9. SPONSORING/MONITORING AGENCY NAME(S) AND ADDRESS(ES)

National Aeronautics and Space Administration
Washington, DC 20546–0001

10. SPONSORING/MONITORING AGENCY REPORT NUMBER

NASA/TM—2005–214192

11. SUPPLEMENTARY NOTES

Prepared by the Spacecraft and Vehicle Systems Department, Engineering Directorate
*Raytheon, Huntsville, AL

12a. DISTRIBUTION/AVAILABILITY STATEMENT

Unclassified-Unlimited
Subject Category 18
Availability: NASA CASI 301–621–0390

12b. DISTRIBUTION CODE

13. ABSTRACT *(Maximum 200 words)*

The Genesis spacecraft reentry represented a unique opportunity to observe a "calibrated meteor" from northern Nevada. Knowing its speed, mass, composition, and precise trajectory made it a good subject to test some of the algorithms used to determine meteoroid mass from observed brightness. It was also a good test of an inexpensive set of cameras that could be deployed to observe future shuttle reentries. The utility of consumer-grade video cameras was evident during the STS–107 accident investigation, and the Genesis reentry gave us the opportunity to specify and test commercially available cameras that could be used during future reentries. This Technical Memorandum describes the video observations and their analysis, compares the results with a simple photometric model, describes the forward scatter radar experiment, and lists lessons learned from the expedition and implications for the Stardust reentry in January 2006 as well as future shuttle reentries.

14. SUBJECT TERMS

reentry, heat shield, entry signatures, Genesis mission, forward scatter radar

15. NUMBER OF PAGES

36

16. PRICE CODE

17. SECURITY CLASSIFICATION OF REPORT	18. SECURITY CLASSIFICATION OF THIS PAGE	19. SECURITY CLASSIFICATION OF ABSTRACT	20. LIMITATION OF ABSTRACT
Unclassified	Unclassified	Unclassified	Unlimited

National Aeronautics and
Space Administration
IS04
George C. Marshall Space Flight Center
Marshall Space Flight Center, Alabama
35812